Hindawi
Advances in Materials Science and Engineering
Volume 2022, Article ID 2000083, 14 pages
https://doi.org/10.1155/2022/2000083

Research Article

Analysis of Rainfall Erosion and Protective Measures for the Aeolian Sand Subgrade Slope of the Wuma Expressway

Wenhua Yin,[1,2] **Fang Wang**,[2,3] **Weizheng Liu**,[4] **Yongxiang Wu**,[5] **and Xu Wang**[1]

[1]*School of Civil Engineering, Lanzhou Jiaotong University, Lanzhou, China*
[2]*Ningxia Highway Survey and Design Institute Co., Ltd, Yinchuan, China*
[3]*Ningxia University, Yinchuan, China*
[4]*Ningxia Highway Administration Center, Yinchuan, Ningxia 750011, China*
[5]*School of Civil Engineering, Central South University, Changsha 410075, China*

Correspondence should be addressed to Xu Wang; publicwang@163.com

Received 15 February 2022; Accepted 11 May 2022; Published 30 May 2022

Academic Editor: Senthil Kumaran Selvaraj

It is difficult to build roads in the desert areas with wind-blown sands because the prevailing harsh environment and the characteristics of the aeolian sands inhibit strategies and measures for road damage prevention and control that are typically effective in other settings. Typically, the rainfall period in aeolian sand areas worldwide is concentrated and the rainfall volume is relatively large, which combined with small and unstable nature and the aeolian sand particles means roads built in these areas can be easily washed away and are vulnerable to water damage. Given geological conditions, topographic features and hydrometeorological conditions differ depending on the region, basic research into water damage in highway roadbed slopes in aeolian sand areas is necessary to formulate treatment measures that are versatile and applicable in different regions. Towards that end, this study strengthens the evaluation of roadbed and pavement drainage and protective measures given aeolian sand erosion caused by rainwater infiltration in certain longitudinal length sections of the Expressway K165 + 250 mileage pile section, and includes verification of the design scheme. The effects of rainwater drainage, storage, and subgrade reinforcement on the seepage and stability of drainage in a long longitudinal slope in the desert hinterland were quantitatively analyzed using numerical analysis. Additionally taking into account the regional climate environment characteristics that locally prevail, the necessity and applicability of geotechnical reinforcement in practical engineering applications is demonstrated. The research found the stability of the subgrade slope given potential for rainfall erosion due to concentrated-rainfall periods in an aeolian sand region is promoted through measures including slope drainage on the highway combined with side ditch drainage, strengthening of the box culvert under embankment ditches, and local protection by laying geogrid in the embankment to produce a significant lateral diffusion effect.

1. Introduction

Aeolian sand is widely distributed in China, with the total area of desertified land reaching about 1.73 million square kilometers by the end of the 20th century, accounting for 17.85% of China's total territory [new1]. According to the latest relevant reports, the desertification land in China mainly concentrated in nine provinces (Heilongjiang, Xinjiang, Gansu, Ningxia, Shaanxi, Inner Mongolia, Qinghai, Jilin, and Liaoning), which belong to the three natural geographic areas–the Qinghai-Tibet plateau, the eastern monsoon region, and the northwest arid area. In China's desert areas, highway transportation has always been the main mode of transportation in aeolian sand areas. Since the new century, with China vigorously advocating the western development strategy and gradually implementing it, it will become very urgent and common to build more roads in aeolian sand areas.

Since the construction of the Yujing Expressway (Yulin-Jingbian expressway, the first expressway in the aeolian sand area in China that opened to traffic in 2003), many roads in aeolian sand areas have been built, providing better

transportation conditions for people in desert areas. However, with more construction of desert roads in China, the problem of road destruction due to water damage has gradually increased. Due to the lack of rainfall in aeolian sand areas, research on the destruction of aeolian sand roads due to water damage in the past is sparse and insufficient. A characteristic of aeolian sand road destruction due to water damage that has led to only slow research progress is the fact that the area with the most severe road destruction by water is not necessarily where water erosion area is driven by the most rainfall, but rather may be an area where wind erosion and water erosion coincide and alternate (dubbed here a "wind erosion and water erosion crisscross area"). When a road is located in a wind erosion and water erosion crisscross area (as has occurred in recent years), it is not uncommon for rainwater from short-lived heavy rain that is collected by drainage ditches to form the back out of the subgrade, directly scouring the natural slope of the aeolian sand. Being formed by windblown sand particles (hence characterized by low viscosity, fine grains, natural moisture content, etc.), the aeolian sand under those conditions can easily be eroded, leading to gradual yet continuous upward erosion that will hollow out the expressway subgrade slope and result in its destruction.

The prevention and control of highway water damage has always been a difficult problem worldwide, resulting in numerous studies in this area of research. Devising prevention and control measures and strategies is already difficult based on the effect of intermittent yet high-intensity rainfall events on the road waterlogging formation mechanism and its effect on the aeolian sand erosion and its effect on the local road damage [1, 2]. Furthermore, the distinguishing features and geological conditions of the road site, terrain hydrometeorological conditions, prevailing highway grade standards, and the waterlogging prevention and control of the structure set already in place, as well many other factors, make linear association between rainfall events and road destruction exceedingly difficult. While scholars at home and abroad have conducted numerous studies on the erosion of roadbed slope reflecting the breadth of diversity worldwide in the erosion scenarios that prevail locally [3–7], the scarcity and infrequency of rainfall in most deserts has resulted in few studies on water damage in aeolian sand areas. The key to the destruction of aeolian sand lies in sediment activation caused by concentrated water flow on the slope [8–10]. Sediment initiation is a complex and variable process that is affected by many factors, such as the nature of the sediment, topography, vegetation coverage, and human activities [11, 12]. At present, although scholars at home and abroad have conducted many studies on sediment initiation [13–15], there are still many problems that need further consideration before knowledge or models of sediment initiation can reliably contribute to the prevention and control of water damage on highways in China and worldwide.

This study focuses on the slope erosion in aeolian sand caused by rainwater infiltration in certain longitudinal length sections of the mileage pile number section of Wuma Expressway K165 + 250 under different rainfall intensities [16, 17]. The assessment of slope erosion further incorporates the meteorological data of the site, to strengthen the evaluation of the roadbed and pavement drainage and protective measures effect and to enable the verification of the design scheme. In this manner, the drainage of representative long longitudinal slopes in desert hinterlands was quantitatively analyzed, in which the influences and effects of rainwater collection, storage, and utilization can also be involved and some regular results can be obtained. Combined with the regional climate environment characteristics of desert hinterlands, the effect of geotechnical reinforcement is also evaluated, and the necessity and applicability of this measure in practical engineering applications is demonstrated.

2. Basic Information of Supporting Projects

As shown in Figure 1, around the road mileage of K163 + 250 in the design documents of the bid section A9 of Qingtongxia-Zhongwei section of Wuhai-Maqin highway (In Ningxia Autonomous Region), a kind of multichannel HDPE sand barrier, a high vertical large sand mesh barrier, a windbreak, sand-fixation forest, and an evergreen shrub forest belt windbreak were installed to protect the sand-fixation roadbed. When encountering 6 m × 3 m box culvert passes through from below perpendicular to the longitudinal of the road, the filling and excavation height of the section is up to 4.876 m, the longitudinal slope gradient is 3.6%, and the slope length is 720 m. For the filling slope, the slope gradient is 1 : 4. When the slope height is greater than 2.5 m, a stepped two-stage slope is adopted. A leveling belt is set at the slope at 2.5 m, and the lower slope is to the bottom. For the test, the main particle size of the aeolian sand in this section is 0.075–0.25 mm, the natural water content of the 0–20 cm dry sand layer is 0.3%–0.5%, and the stable water content of the following sand layer is 1%–3%. The critical wind speed was determined to be 4.1 m/s, the natural angle of repose of the sand was 37°, and the angle between the dominant wind direction west (W) wind and the route direction is 20–60°. According to the design data, roadbed drainage is scattered drainage, road drainage of the slow slope road water is also scattered drainage. No water curb stone or rapid groove was presumed, soil shoulder was created using M10 cement mortar hand pebble reinforcement, and filling the slow slope is mainly used in the main line and overpass ramp slope protection using concrete frame pressure covered pebble protection. Figure 1(b) shows the cross section of the design standard of the general filled roadbed.

Figure 2 shows the rainfall in this region mainly occurs in June, July, and August, with the highest rainfall intensity reaching 33.8 mm. Meteorological data of this section of the desert highway from May 2020 to January 2021 was collected, screened, and analyzed, and three typical cases with small, medium, and large rainfall were identified for consideration; the cases are listed in Table 1. The case of heavy rainfall was selected for modeling analysis.

3. Analysis of Rainfall Erosion and Water Damage

For common highway drainage designs, drainage grooves, side ditches, and box culverts are usually set up on the roadbed slope. In sandstorm areas, precipitation is scarce

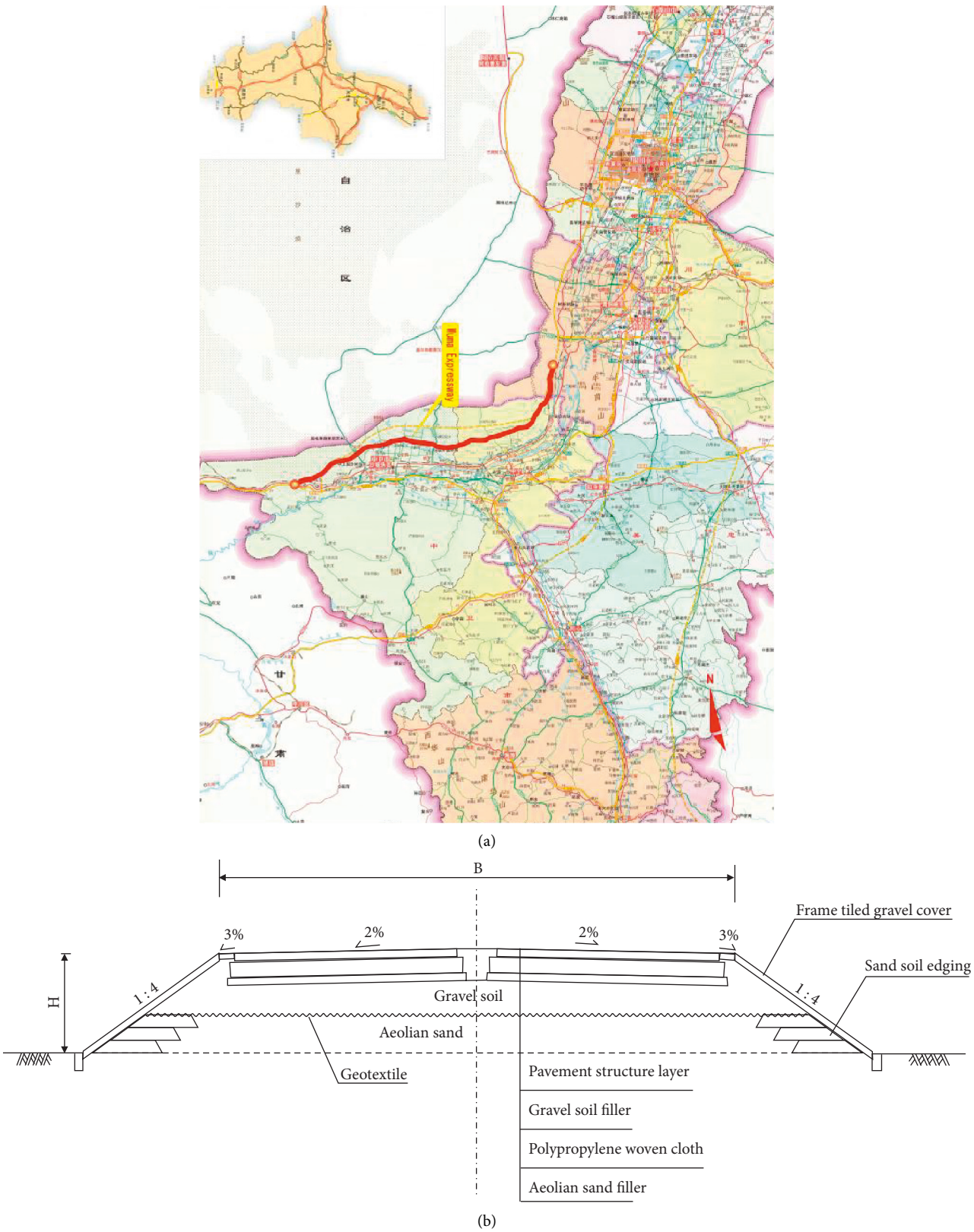

Figure 1: Background information of relying project. (a) Schematic of the location of the section in the study area. (b) Standard cross-section diagram of roadbed.

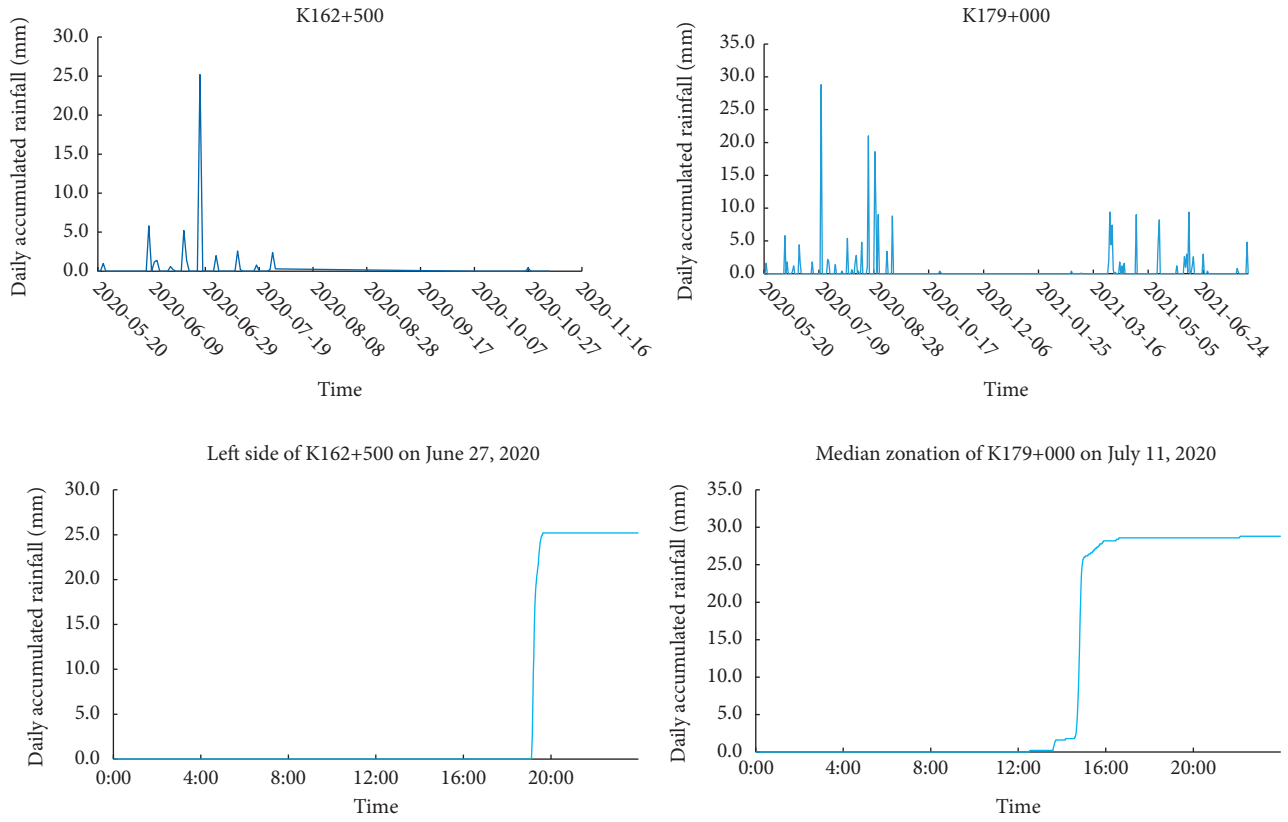

Figure 2: Statistical analysis of rainfall in Wuma expressway.

Table 1: Rainfall summary.

Date	Cumulative rainfall (mm)	Heavy rain speed (mm/min)	Rain event duration (h)
2020/7/24	1.8	0.05	4
2020/8/23	33.8	0.8	12
2020/9/14	8.2	0.6	1.5

and sand permeability is good, therefore drainage facilities are generally not considered necessary. Such presumed adequacy of minimalist drainage is folly; however, since heavy rain produces the overflow phenomenon. The slope from the Expressway shown in Figure 3 appears to have suffered serious water damage, which is consistent with engineering experience that has found roadbed water damage to be one of the common diseases of desert highways. As shown in Figure 3, according to the field investigation conducted for the Wuma high-speed waterlogging situation analysis, culverts damaged by flood drainage holes and damage cracks fall into these three categories: the aeolian sand region of waterlogging due in most part to the heavy rainfall flood season; the flow formed after rainwater confluence directly contacts the unprotected aeolian sand slope; the soil around the box culvert being more likely to produce erosion damage. The erosion damage is usually caused by the rill first; with the formation of the rill, the rill becomes deeper and wider, turning into a gully. The gully is constantly cut and destroyed, leading to the destruction of the roadbed slope.

Aeolian sand is a special type of soil that is different from common cohesive soil, in that it has poor stability and is easily eroded and scoured by current. If heavy rainfall continues, the transformation from rill formation stage to subgrade slope scouring failure stage will be completed in a short time. Because of the special physical properties of aeolian sand, the gully section of an uncompacted natural slope is generally an inverted trapezoid during gully formation and development. Owing to the compaction of the aeolian sand embankment slope, the gully has the characteristics of a steep wall and narrow section. With further erosion, the side edge of the roadbed slope is eroded at the bottom of the gully, which leads to the gully walls becoming suspended in air without support from underneath; the gully wall collapses in strips, which leads to further widening of the gully. Because the flow out in a straight line is the shortest and fastest means of hydraulic energy dissipation, the axis of the gully is generally linear on the slope and then follows the natural slope of the aeolian sand roadbed. The water damage of subgrade slope in aeolian sand area is the inevitable result of rainfall centralized drainage. The causes of water damage include both internal defects (internal causes) and external effects (external causes). No matter what form of water damage, as long as it occurs in aeolian sand area, it has the characteristics of short duration, rapid development, and great damage. We should be vigilant in the early stage of project construction.

Figure 3: Picture of drainage ditch water damage site.

Modeling analysis was performed in this study using the finite element analysis method, with the Mohr-Coulomb constitutive model used for the soil mass. As groundwater is deep in desert areas, groundwater is set at the bottom of the model (at a depth coordinate of −40 m), and the grid size is fine, with 16,127 elements and 24,231 nodes in total; the model mesh is shown in Figure 4. The physical and mechanical parameters of this model were selected based on information from the relevant engineering geological surveys, drilling, in-situ tests, and laboratory tests, combined with site engineering geological conditions. The precipitation is shown in Table 2. The soil and water characteristic curves were automatically generated by the software, where K is the relative permeability coefficient, and S is the saturation; it can be found that when the saturation is 20%, the matric suction head is 0.2 m and the relative permeability coefficient is 0.0001.

Rainfall intensity can be implemented by setting the flow rate per unit time, simulating only the slope with all rainfall infiltration, eliminating the possibility of slope runoff, and water accumulation. In the actual rainfall situation, due to the limitation of rainfall intensity and the rate of slope infiltration, infiltration can be roughly divided into three situations as listed below.

(1) When the rainfall intensity is less than the slope permeability, rainwater can penetrate into the interior of the slope body.
(2) When the rainfall intensity is greater than the slope permeability, part of the rain penetrates into the slope body, and part of the water will form on the surface of the slope. The water reaches a certain level, it is connected to form slope runoff; at this time, it is necessary to use external drainage measures to assist drainage.
(3) When the surface soil of the slope has permeated and saturated, the permeability coefficient of the slope soil is close to zero, and rainwater cannot penetrate the slope body. This situation will also form surface runoff, and rainwater will not continue to penetrate the slope body.

The total rainfall of the two working conditions in the table above is the same, with the rainfall intensity for the second condition twice that for the first condition. Short-term rainstorms and long-term rainfall can be compared in desert areas to comprehensively simulate the stable

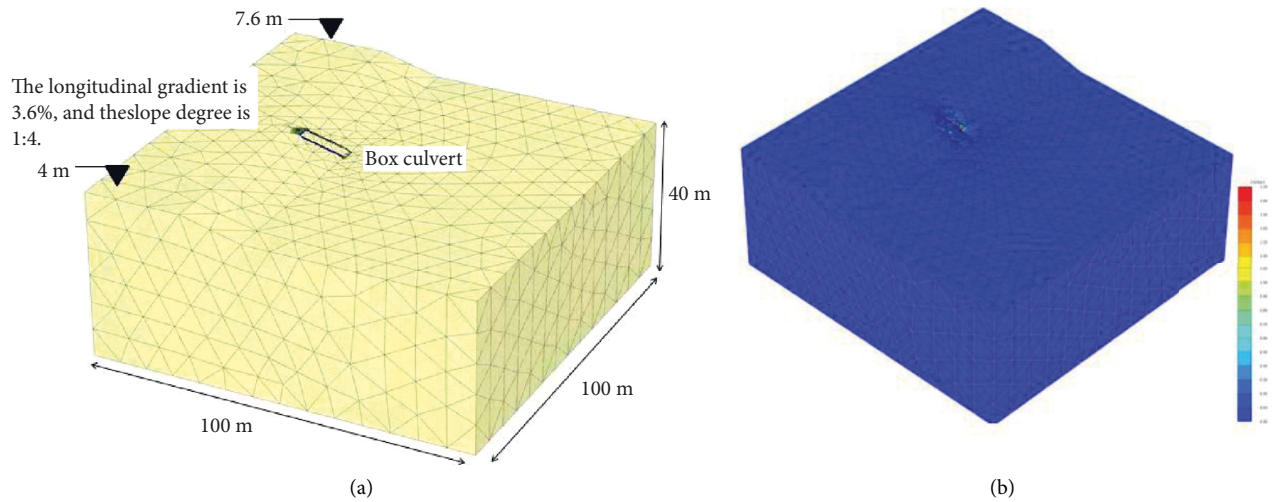

Figure 4: Construction model of embankment slope analysis section. (a) Model diagram. (b) Rainfall infiltration seepage field.

Table 2: Simulated working condition of rain condition.

Rainfall intensity (mm/d)	Rainfall time (h)	The total rainfall (mm)
38.8	6, 12, 24	9.7, 19.4, 38.8
77.6	3, 6, 12	9.7, 19.4, 38.8

condition of the slope under different rainfall amounts and rainfall intensities. The overall rainfall infiltration cloud map of the model is shown in Figure 4(b). It can be seen that rainwater infiltration is evenly distributed on the surface, which conforms to reality and indicates that the rainfall simulation is effective. After the rainfall simulation, the safety and stability of the rainfall results were analyzed to calculate the deformation of the entire slope, safety factor, sliding surface depth, and other parameters.

The left figure of Figure 5 shows the vertical pore water pressure distribution curve of the embankment with a rainfall intensity of 38.8 mm for different durations. In the initial stages, the pore water pressure exhibited a linear distribution. With the increase in rainfall duration, the pore water pressure gradually decreased, the suction gradually decreased, and the surface soil gradually became saturated. The influence range was approximately 15 m below the slope top. The figure on the right of Figure 6 shows the vertical pore water pressure distribution curve of the embankment when a rainfall intensity of 77.6 mm prevailed for different durations. It can be seen from Figure 7 that under heavy rainfall, the pore water pressure decreases with the increase in rainfall time and the suction decreases, which is significantly different from that under the first working condition: (1) the rainwater infiltration depth is approximately −10 m, which is 5 m smaller than that under the first working condition. (2) The decrease in pore water pressure was concentrated in the shallow layer. The above conclusion indicates that the surface soil is more easily saturated under the condition of short-term rainstorms, and there is no necessary relationship between the infiltration depth of rainwater and seepage rate.

This is mainly because when rainfall-type landslides occur under rainfall infiltration and a combination of the two (infiltration and seepage), the slope soil mass balance is destroyed, resulting in a downward sliding phenomenon. For aeolian sand under the effect of rain infiltration, the sharp decline in the strength results in aeolian sand erosion, where landslides are often triggered and proceed in a flash. The mechanism of landslides caused by rainfall can be understood as follows: rainfall infiltration increases the water level of the slope, softens the soil at the sliding surface, and reduces the shear strength, thus reducing the stability of the slope. In addition, rainfall infiltration increases the weight of the slope soil, which further increases the driving force of the landslide and reduces the safety factor of the slope. The strength reduction method is used to analyze the stability of the rainfall infiltration-induced slope in the above model, and the slope sliding surface properties obtained are shown in Figure 8.

According to the model calculation, the sliding surface depth is about 3.2 m when the rainfall intensity is 38.8 mm/d, and 1.4 m when the rainfall intensity is 77.6 mm/d. The short-term rainfall rate is fast, and rain mainly concentrates on the soil surface. Long-term rainfall, although of lower intensity, can still seep into the deeper soil layer, which can make the soil strength within the range of the rain infiltration surface drop greatly, leading to slope landslides. Therefore, in the case of the same rainfall, heavy rain is more likely to produce surface runoff and thus wash the slope, but attention should also be paid to the deep slope slip under the condition of long light rain.

Figure 9 shows a comparative analysis of the numerical simulation results and on-site water damage. The damage is visible and more concentrated in the box culvert side fields waterlogging area, with deep gullies and a large gully area indicative of extensive waterlogging. In addition, more water

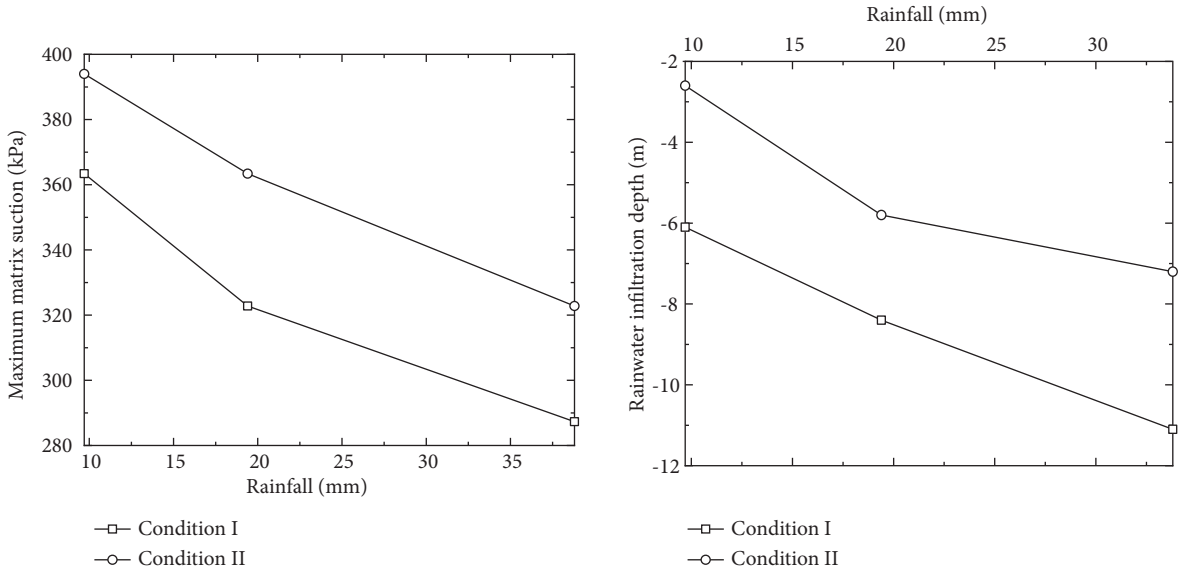

Figure 5: Changes of matrix suction and rainwater infiltration.

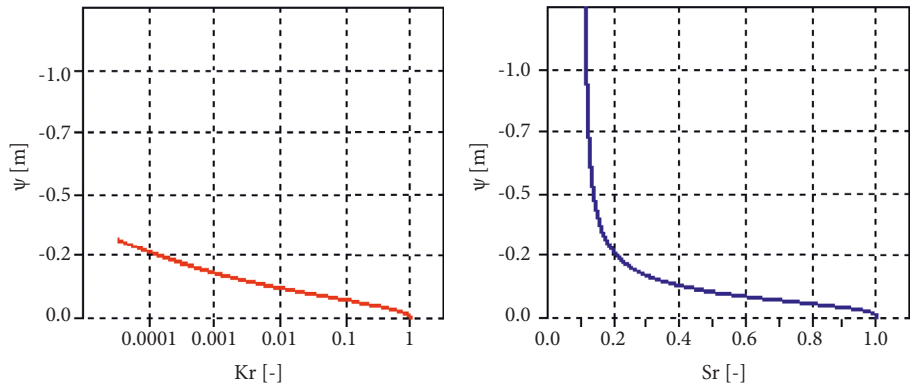

Figure 6: Soil water characteristic curve used in model construction.

comes out of the culvert, indicating that the regional rainfall intensity is high, making the slope surface runoff and rainfall infiltration of slope also high; this has a larger impact on the stability and safety of highway embankments.

4. Drainage Measures and Effect Evaluation

The main mechanism of measures to control water damage is to improve the anti-scour ability of slope surface soil and increase the drainage capacity of the highway as a whole. In this study, a numerical analysis was used to calculate the effect of the drainage facilities of a high-speed slope. The calculation results show that the drainage facilities have a significantly improved slope water damage, i.e., reducing it. The Wuma high-speed drainage system is composed of slope drainage and slope-foot collecting ditches. This drainage system collects slope rainwater, and recycles it, effectively using desert water resources for vegetation irrigation. This water re-use method completely conforms to the design concept of a green highway. The two types of drains are analyzed in detail below.

To reduce slope rainwater infiltration, slope drainage ditches need to be set on the slope on-site. Two slope drainage ditches are set based on the original model, with a width of 0.2 m, rainfall of 33.8 mm, rainfall rate of 77.6 mm/d, and rainfall duration of 12 h. The model mesh is illustrated in Figure 10. After the drainage ditch is set on the slope, the rainwater infiltration depth decreases significantly, from 7.2 m to 5.1 m, and the closer it is to the drainage ditch, the smaller the infiltration depth is. There is no rainwater infiltration below the drainage ditch, the rainfall infiltration area on the slope is reduced, and the local infiltration rate will be large. This is due to the existence of slope drainage, which makes the seepage concentrated. There are some defects in using slope drainage only. Slope drainage only reduces the rainwater infiltration depth outside the pavement, while the rainwater infiltration in other locations is still very obvious. The short-term rainwater infiltration depth is small. With the passage of time, rainwater will penetrate into deeper soil and soften the soil on the sliding surface. It can be seen that only setting the slope drainage can keep the slope in a safe state for a short time, but it

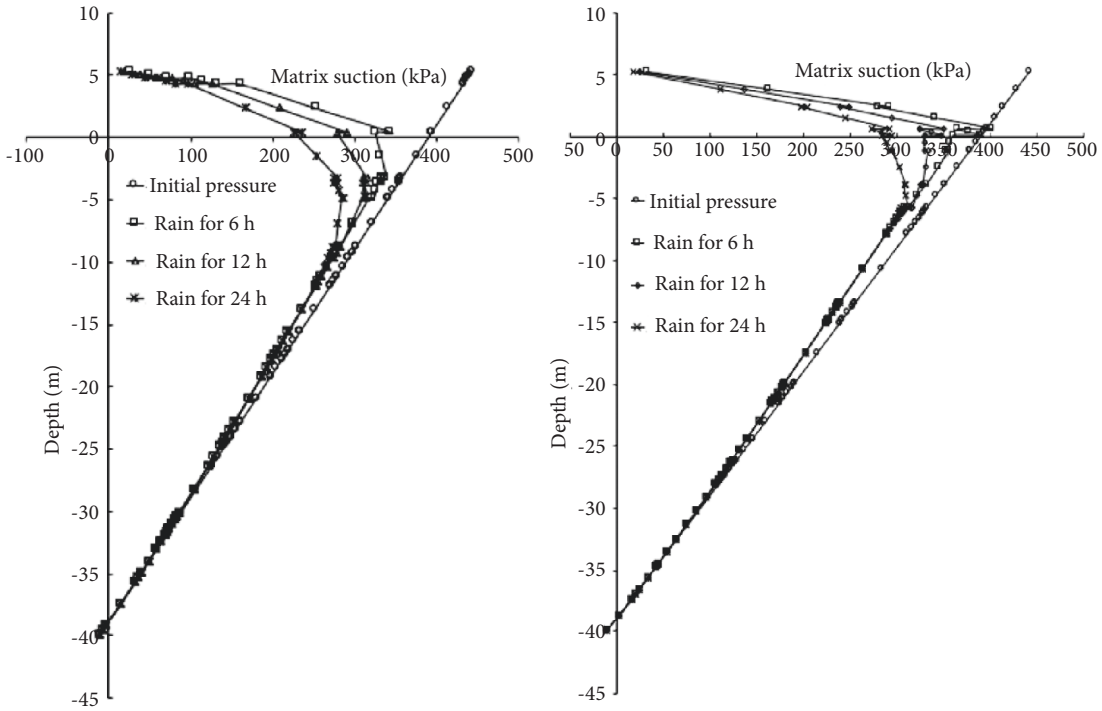

Figure 7: Variation of rainfall infiltration suction depth.

Figure 8: Stability analysis of potential sliding surface of slope. (a) Rain strength 38.8 mm/d. (b) Rain strength 77.6 mm/d.

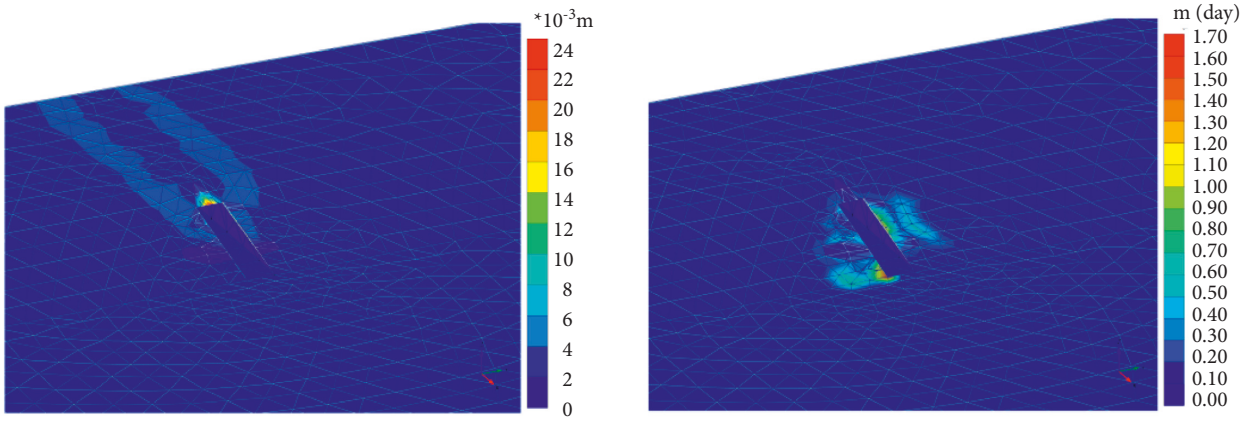

Figure 9: Continued.

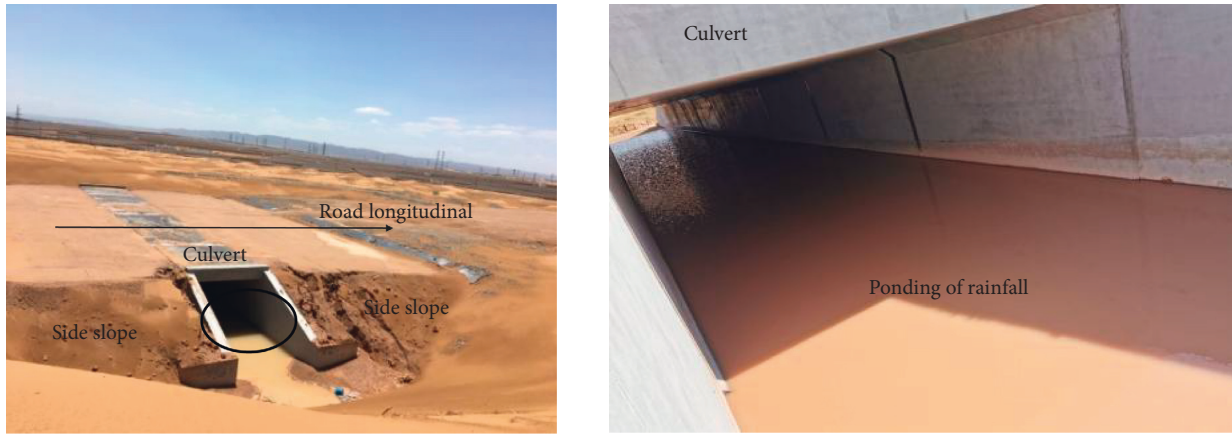

(c) (d)

Figure 9: Site water damage of slope at box culvert. (a) The deformation field. (b) Seepage field. (c) Slope erosion. (d) Box culvert bottom water.

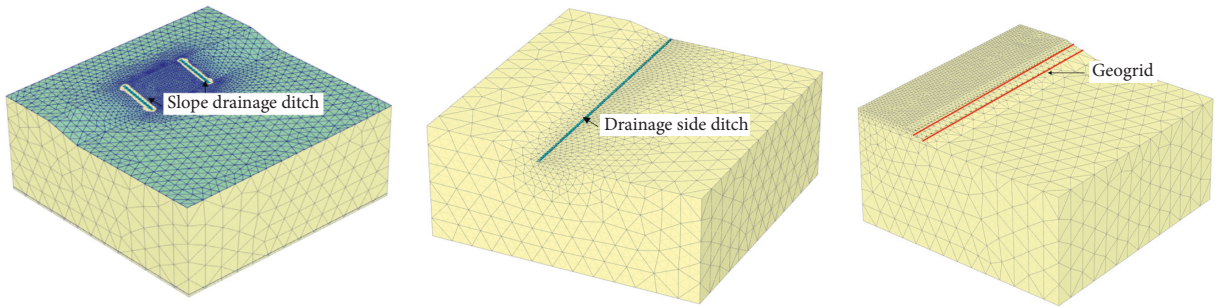

(a) (b) (c)

Figure 10: Three different slope protection measures. (a) Slope drainage. (b) Bottom edge. (c) Geogrid reinforcement.

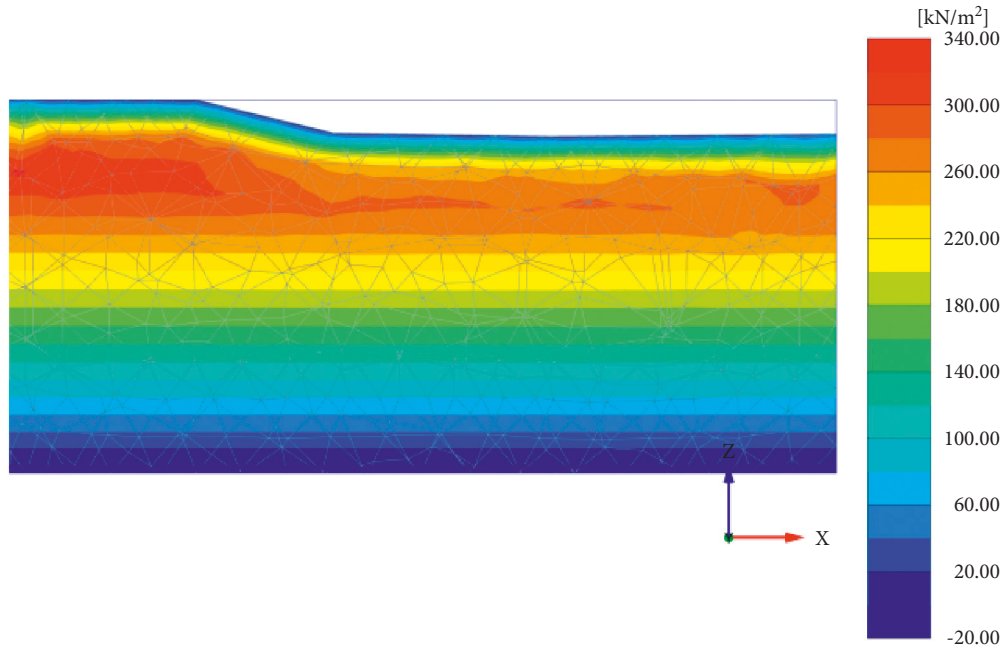

(a)

Figure 11: Continued.

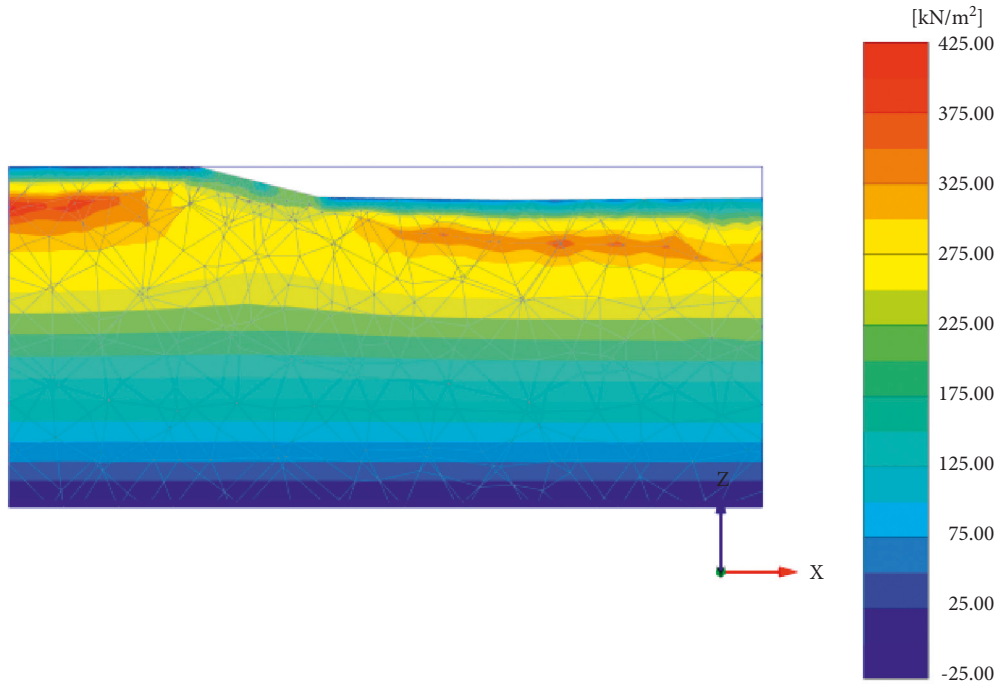

(b)

Figure 11: Cloud map of pore water pressure of slope drainage ditch.

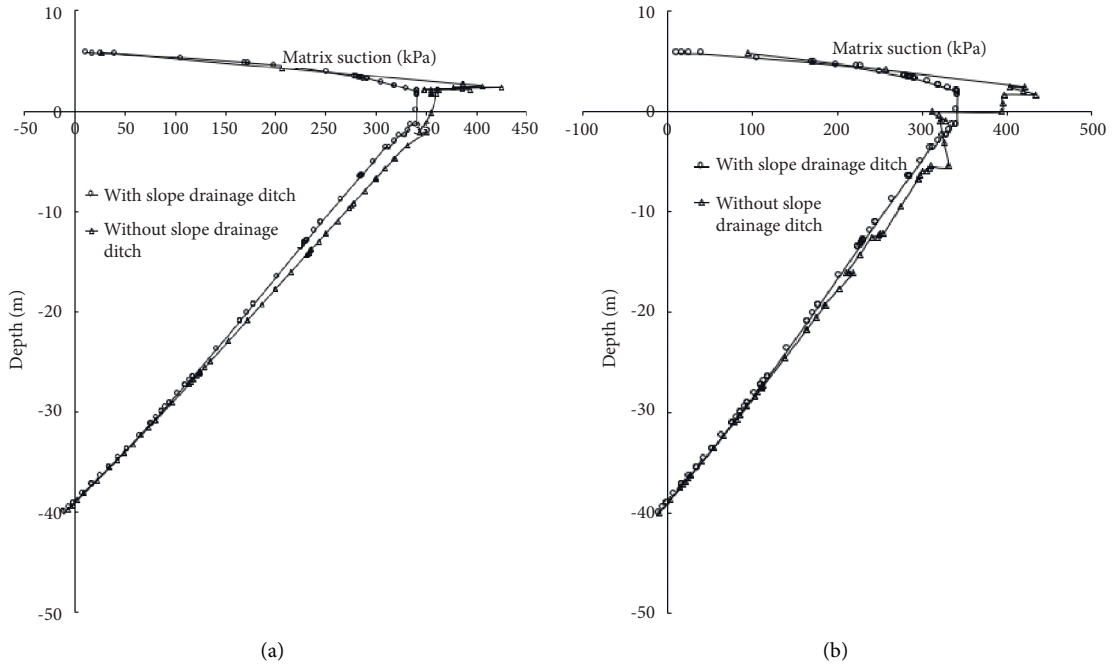

(a) (b)

Figure 12: Influence of drainage conditions on pore water pressure. (a) There is no drainage groove. (b) There is no drainage-side channel.

cannot fundamentally solve the problem of rainwater infiltration.

As shown in Figures 11 and 12, the drain is set up after the pore water pressure is greater than in the original state. With the increase in suction and low surface moisture content (compared to when no drainage measures are in place), embankment slope stability increases: the set maximum pore water pressure is 425 kPa, while without the drain the maximum pore water pressure is 340 kPa. The drain can thus reduce pavement rainwater infiltration,

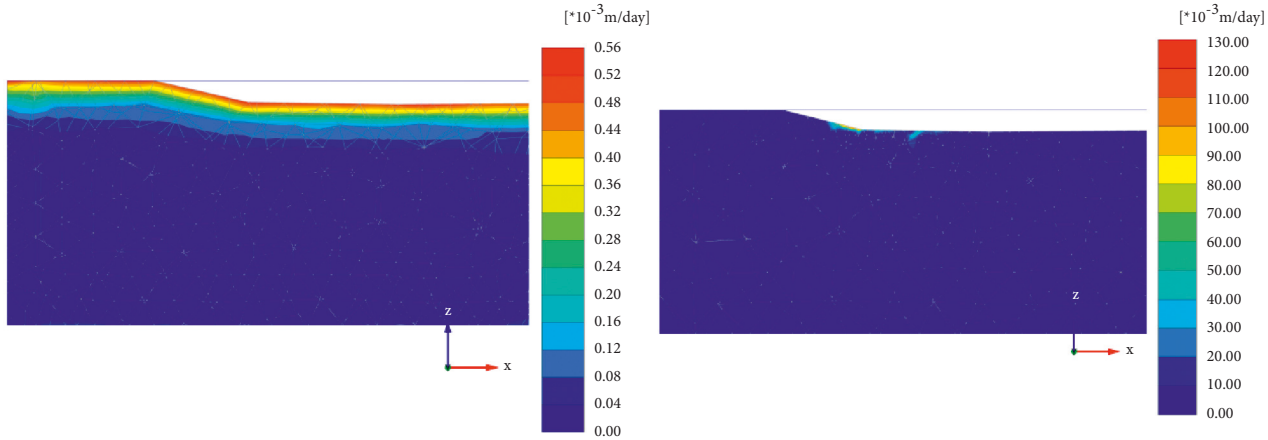

Figure 13: Cloud map of seepage field of drainage ditch at slope toe.

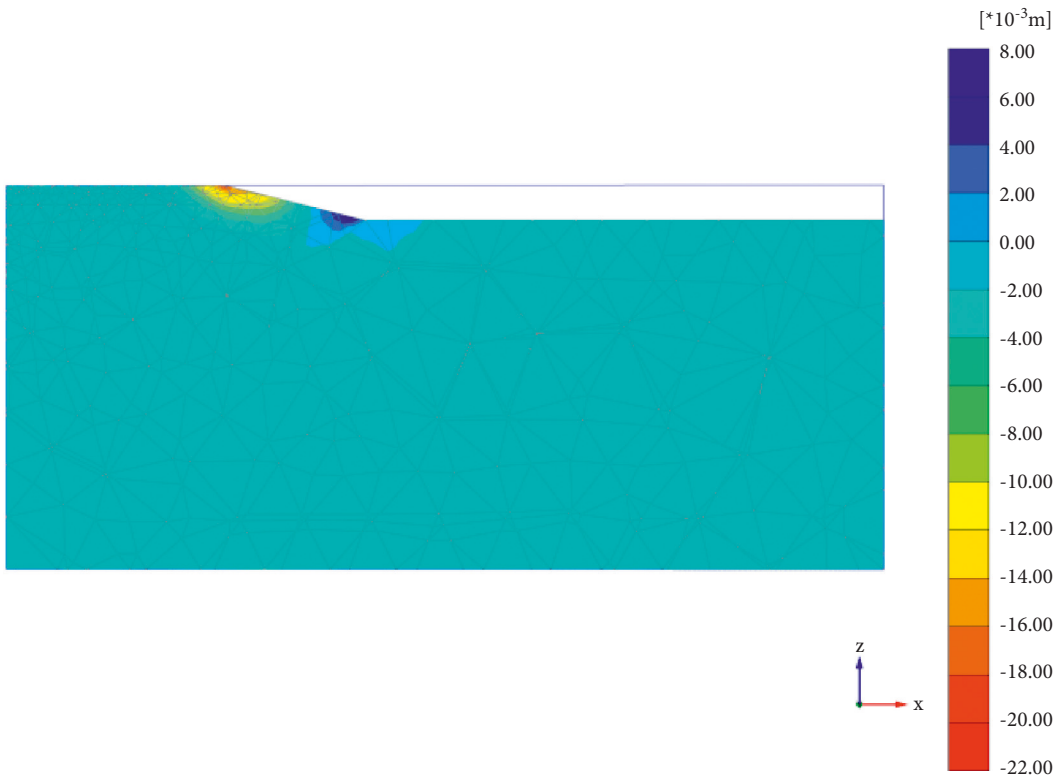

(a)

Figure 14: Continued.

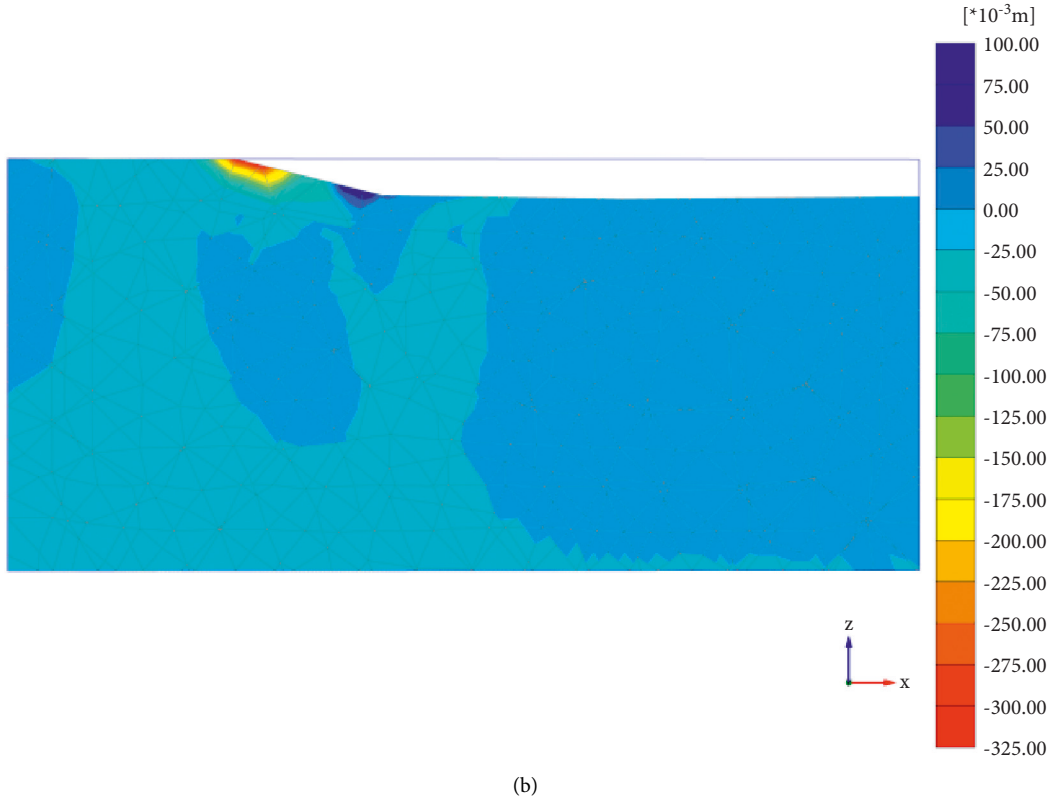

(b)

Figure 14: Deformation nephogram with or without grid. (a) No grid displacement cloud image. (b) Grid deformation cloud image.

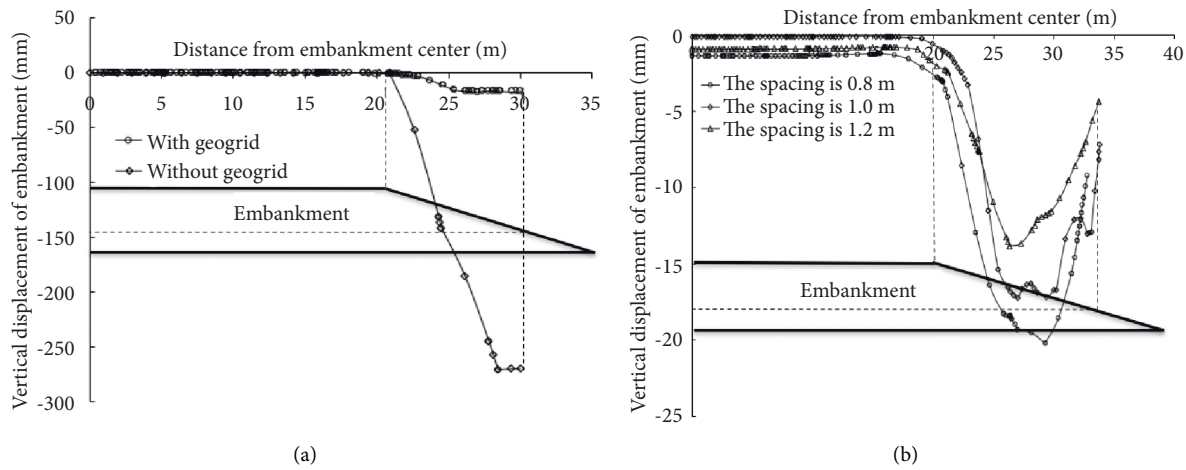

(a) (b)

Figure 15: Position effect analysis of geogrid reinforcement. (a) Presence of reinforced. (b) Muscle layer spacing.

which is beneficial for improving the degree of water damage of the embankment slope, although it is not suitable for long-term treatment.

As shown in Figure 13, the drainage effect of the drainage ditch is better. In addition to the drainage ditches surrounding areas with rain infiltration, the rain infiltration elsewhere is basically negligible. The slope and the slope drainage only reduce the rain infiltration. There is still more rain infiltration: while the rest of the drainage ditches make up for the shortcomings, there are some limitations when only the drainage-side ditches exist. This method will lead to a concentration of rainwater seepage, which will increase the seepage velocity of soil water around the side ditch. Over time, it may cause erosion and destruction of the soil around the side ditch.

After setting drainage ditches, shallow matrix suction increased significantly, which shows that the drainage ditches can effectively reduce rainwater infiltration. The drainage ditch drainage effect in that case is more obvious, with the slope surface and the surface below 5 m within the

scope of the matrix suction declining obviously due to the existence of drainage ditches. This will be a big part of rainwater discharged in time, given the amount of rainwater infiltration is small and most of the infiltration is only around the drainage ditch. With the drainage ditches, the existence of the rainfall infiltration area is concentrated around the edge; the farther from the edge, the smaller the pore water pressure at the top of the slope. The slope did not reach saturation, and the drainage ditches could effectively reduce the amount of rainfall infiltration of the slope, but the lateral slope and slope toe area rainfall amount is larger, along with the saturation being larger which may produce surface runoff.

Figure 14 shows the vertical displacement cloud diagram of the slope with and without the geogrid. The reinforcement effect of the geogrid is very obvious, as can be deduced given the following observations: (1) the amount of slope subsidence is significantly reduced; (2) the settlement deformation is initially distributed on the entire slope, except for upward displacement at the foot of the slope. After the addition of the geogrid, the area of settlement deformation on the slope is significantly reduced. Vertical deformation occurs from the elevation of the lowest geogrid as the starting point, while the vertical displacement of the soil below the elevation to the foot of the slope is very small.

As shown in Figure 15, the vertical displacement of the embankment caused by rainfall was mainly concentrated on the slope surface, and the settlement of the embankment surface was small. Compared with the settlement of the slope surface, the settlement of the pavement can be ignored. In the absence of a geogrid, the slope settlement was 26 cm, and the settlement decreased obviously after the addition of geogrid. Therefore, it can be seen that the reinforced embankment plays a significant role in reducing the slope settlement, and the reinforced effect of the geogrid on the highway embankment is more significant because the embankment is slow and the settlement is larger. Three working conditions with geogrid spacing of 0.8 m, 1 m, and 1.2 m were considered. The vertical settlement of the road surface varied little under the three types of spacing. When the spacing was 1 m, the vertical settlement of the road surface was the minimum attained, and when the spacing was 0.8 m, the vertical settlement was the maximum attained, while the main settlement was concentrated on the slope. According to the slope settlement curve, the settlement is the minimum when the spacing is 1.2 m and the maximum when the spacing is 0.8 m. The distance between the geogrid should be selected according to the actual working conditions.

5. Conclusions

In closing, it is possible to document five key conclusions to come out of this work.

(1) With the increase of rainfall duration and rainfall intensity, the water content of slope soil gradually increases, the shear strength of soil decreases, and the overall anti-sliding stability of slope decreases. The simulation analysis shows that when the rainfall remains unchanged and the rainfall intensity increases, the slope stability coefficient gradually decreases, which has a significant impact on the stability of the slope. There is also the problem of water damage. It is necessary to consider adding slope drainage measures and strengthening displacement and deformation monitoring.

(2) It is also found that the rainwater seepage field is mostly concentrated on both sides of the box culvert, and the seepage rate is large. The soil on both sides of the box culvert is vulnerable to rainwater infiltration erosion. It is necessary to consider adding slope drainage ditches on both sides of the box culvert. It is suggested to consider the drainage measures combining slope drainage and side ditch drainage to further optimize the slope drainage system.

(3) Laying geogrid in the embankment can better restrain the subgrade slope displacement. For this working condition, the reinforcement effect is better when the geogrid spacing is 1.2 m. In order to take preventive measures, it is recommended to pave multilayer geogrids at large positions of box culverts and slopes and set up a variety of drainage measures to reduce the hazards of water damage and slope instability.

Data Availability

Some data, models, or code generated or used during the study can be obtained from the corresponding author upon request.

Conflicts of Interest

The authors declare that there are no conflict of interest regarding the publication of this paper.

Acknowledgments

This study was funded by Department of Transportation of Ningxia (Grant No. 20200173) and Ningxia Science and Technology Department (Grant No. 2021BEG02017).

References

[1] W. Boqiang, W. Yong, and Y. Dehong, "Main geologic engineering issues and geologic route selection of jinwu highway," *Subgrade Engineering*, vol. 3, pp. 44–49, 2021.

[2] Q. Ning, Z. Bin, X. Fengquan, R. Zhijun, and W. Zhixiang, "Application of the experiences obtained from the yangwu irrigation district in dealing with the sediment problem of low-head diversion works," *Journal of Sedimentary Research*, vol. 2, pp. 1–9, 1983.

[3] B. Kumar, G. Srinivasulu, and A. R. Rao, "Incipient motion design of sand bed channels affected by bed suction,"

Computers and Electronics in Agriculture, vol. 74, no. 2, pp. 321–328, 2010.

[4] S. R. Benik, B. N. Gilson, D. Biesboer, B. Hansen, and D. Stenlund, "Performance of erosion control products on a high gay embankment," *Transactions of the American Society of Agricultural Engineers*, vol. 46, pp. 1113–1119, 2003.

[5] M. A. Casermeiro, J. A. Molina, M. de la Cruz Caravaca, J. Hernando Costa, M. I. Hernando Massanet, and P. S. Moreno, "Influence of scrubs on runoff and sediment loss in soils of Mediterranean climate," *Catena*, vol. 57, no. 1, pp. 91–107, 2004.

[6] E. Chirino, A. Bonet, J. Bellot, and J. R. Sánchez, "Effects of 30-year-old Aleppo pine plantations on runoff, soil erosion, and plant diversity in a semi-arid landscape in south eastern Spain," *Catena*, vol. 65, no. 1, pp. 19–29, 2006.

[7] S. Dey, "Experimental study on incipient motion of sediment particles on generalized sloping fluvial beds," *International Journal of Sediment Research*, vol. 16, no. 3, pp. 391–398, 2000.

[8] J. L. Pikul, J. K. Aase, and J. K. Aase, "Water infiltration and storage affected by subsoiling and subsequent tillage," *Soil Science Society of America Journal*, vol. 67, no. 3, pp. 859–866, 2003.

[9] Z. Luyu, Z. Yingren, Z. Shang, Z. Shangyi, and S. Weimin, "The feasibility study of strength reduction method with FEM for calculating safety factors of soil slope stability," *Journal of Hydraulic Engineering*, vol. 1, pp. 21–27, 2003.

[10] Z. Zihao, S. Zhandong, W. Chenglong, and W. Jing, "Compaction degree control method of aeolian sand modified soil samples," *Journal of China & Foreign Highway*, vol. 41, pp. 264–268, 2021.

[11] Z. Hong, L. Hairyang, and L. Cong, "Temperature effect of soil-water on characteristic curve of aeolian sand subgrade soil," *China Journal of Highway and TransportChina J. Highw. Transp*, vol. 33, no. 7, pp. 42–49, 2020.

[12] B.-B. Zhang, J. Liu, A. Tohuti, W. Bin, and A. Yuhao, "Field experimental study on dynamic stress response of aeolian sand subgrade strengthened by geocell," *Journal of Highway and Transportation Research and Development*, vol. 38, no. 12, pp. 37–46, 2021.

[13] L. Chi and W. Jianhua, "Model testing study and calcuiating analysis of bearing capacity on the reinforced aeolian sands ground," *Chinese Journal of Rock Mechanics and Engineering*, vol. 24, no. 4, pp. 687–691, 2005.

[14] L. Weihua, L. Weizheng, S. Xin, and Z. Jizhou, "A tensile strain analysis approach for basal geosynthetic reinforcement based on different working section mode," *Journal of Railway Science and Engineering*, vol. 18, no. 5, pp. 1155–1167, 2021.

[15] Z. Rui, L. Hai yang, and Z. Hong, "Analysis on influence factors of matric suction of aeolian sand filled subgrade soil," *Highways*, vol. 3, pp. 47–53, 2021.

[16] Y. Wenhua, W. Xu, Z. Jizhou, L. Weizheng, and M. Xuening, "Experimental study on compaction characteristics and filling method of subgrade aeolian sand for expressway in desert hinterland," *Journal of Railway Science and Engineering*, vol. 18, no. 5, pp. 1177–1187, 2021.

[17] Y. Wenhua, W. Xu, Z. Yichen, L. Zhibo, and L. Liangying, "Design of desert geospatial database based on GIS," *Journal of Lanzhou Jiaotong University*, vol. 40, no. 4, pp. 7–12+36, 2021.